Photoluminescence Characteristics of Al_2O_3/Si Multilayer Structures Fabricated by DC Reactive Sputtering Technique

Haneen H. Shaaban, Mohammed A. Hameed

Department of Physics, College of Science, University of Baghdad, Baghdad, Iraq

Abstract

In this work, the photoluminescence (PL) characteristics of the multilayer structures fabricated from Al_2O_3 thin films deposited on silicon substrates with varying film thicknesses were introduced and studied. The PL spectra indicate multiple emission peaks, suggesting various radiative recombination pathways. The 250 nm Al_2O_3 sample shows significantly higher PL intensity and distinct peak shifts compared to other thicknesses, implying an optimal thickness for enhancing radiative recombination. Shifts in peak positions and intensity variations with Al_2O_3 thickness are attributed to quantum mechanical effects, such as quantum confinement, and the influence of interface quality or defects. The results presented herein highlight the critical interplay between Al_2O_3 layer thickness, material defects, and the resulting optical properties of these multilayer structures.

Keywords: Aluminum oxide; Photoluminescence; DC sputtering; Multilayer structures
Received: 18 June 2025; **Revised:** 21 July 2025; **Accepted:** 28 July 2025; **Published:** 1 October 2025

1. Introduction

Reactive magnetron sputtering is a versatile and reliable technique for preparing thin films, including nanostructured Al_2O_3. This method involves introducing a reactive gas, such as oxygen, which reacts with the sputtered target material to form a compound film [1-3]. A key advantage of reactive sputtering lies in its ability to precisely control the film's properties by optimizing parameters like oxygen partial pressure, DC power, working gas pressure, and substrate temperature. This fine control is particularly beneficial for fabricating multilayer structures, where distinct layers with tailored compositions and properties are required [4-6]. By sequentially depositing different materials or varying reactive gas compositions, sophisticated multilayer stacks can be achieved, enabling the creation of advanced devices with enhanced functionalities [7]. The technique allows for the deposition of a wide variety of compounds, offering broad applicability [8,9].

Aluminum oxide (Al_2O_3) is a material with diverse applications due to its excellent optical, electrical, and mechanical properties [10]. In nanostructured forms, Al_2O_3 exhibits enhanced characteristics suitable for various fields, including optoelectronics [11]. Preparation methods for Al_2O_3 nanostructures include techniques like atomic layer deposition (ALD), chemical vapor deposition (CVD), and sputtering [12-14]. For optoelectronic applications, Al_2O_3 thin films are valued for their high transparency across a wide spectral range, high dielectric constant, and good insulating properties [1]. These characteristics make them ideal for use as gate dielectrics in thin-film transistors, passivation layers in solar cells, and protective coatings for optical components [2]. Their stability and tunable refractive index also contribute to their importance in fabricating anti-reflection coatings and waveguides in integrated optical devices [10-14].

Multilayer structures fabricated from nanostructures on silicon substrates are critical in numerous practical applications, particularly in microelectronics and optoelectronics [15,16]. Silicon, being a mature and widely used semiconductor, provides a robust platform for integrating various functional layers [17,18]. By depositing nanoscale layers of different materials, such as oxides, nitrides, or metals, precise control over the overall device characteristics can be achieved [19,20]. These multilayer stacks enable functionalities like enhanced light absorption or reflection, improved electrical insulation, optimized charge transport, and superior protection against environmental degradation [21,22]. Examples include advanced gate stacks in transistors for higher performance, anti-reflection coatings on silicon solar cells for increased efficiency, and complex optical filters for sensing applications [23,24]. The ability to engineer properties at the nanoscale within these multilayer architectures is fundamental to the continued advancement of high-performance electronic and photonic devices [25-27].

2. Experimental Part

A DC reactive magnetron sputtering system was employed in this study to prepare Al_2O_3 thin films on silicon substrates. A high-purity (99.99%) aluminum sheet served as the sputtering target in the presence of oxygen. Prior to deposition, both the targets and the substrates were thoroughly cleaned and dried. The aluminum target was securely mounted on the cathode, and the plasma required for sputtering was generated by an argon discharge. A high-voltage DC power supply capable of delivering up to 5 kV provided the necessary electrical power.

The mixing ratio of argon and oxygen gases was 50:50. Initially, the deposition chamber was evacuated to a base pressure of 0.001 Torr. The films were deposited at room temperature, under a discharge voltage of 650–700 V and a discharge current of 25 mA. Different deposition times were considered to produce Al_2O_3 films with different thicknesses. The distance between the electrodes was maintained at 4 cm. The optimal discharge current was chosen based on the stability of the plasma discharge. During deposition, the working pressure of the gas mixture was about 0.15 mbar. The gas flow into the chamber was carefully regulated, and the internal temperature was measured with a precision thermometer. Both electrodes could be water-cooled via internal cooling channels to maintain stable operating conditions. Further technical details of the sputtering system are available in references [28-32].

Film thickness was measured by optical interferometry, which relies on the interference of coherent light reflected from the thin film's top surface and the substrate interface, with an estimated measurement error of about 3%. A 630 nm diode laser served as the light source. Film thickness was calculated using the equation [2]:

$$d = \frac{\Delta x}{x} \cdot \frac{\lambda}{2} \qquad (1)$$

where x is the fringe width, Δx is the distance between two fringes, and λ is the laser wavelength. The deposition rate was determined from the variation of film thickness with deposition time, as shown in Fig. (1).

Characterization of the fabricated multilayer structures included UV–visible spectrophotometry and photoluminescence spectra using SpectraAcademy S2200 spectrophotometer.

3. Results and Discussion

Figure (2) illustrates the absorption spectra of the multilayer Al_2O_3/Si structures, fabricated in this work, with varying thicknesses of the Al_2O_3 layer (200, 250, and 325 nm). A prominent feature across all three spectra is a sharp absorption peak observed around 300 nm, indicating strong absorption in the UV region. This intense absorption in the UV range is characteristic of the electronic transitions within the Al_2O_3 material, specifically the band-to-band transitions of aluminum oxide. The position of this peak, while generally consistent, shows slight shifts, which could be attributed to variations in the Al_2O_3 layer thickness or subtle changes in the film's stoichiometry or crystallinity induced by the sputtering process. As the wavelength increases beyond the UV region into the visible spectrum, the absorbance dramatically decreases for all samples, suggesting that these Al_2O_3/Si structures are relatively transparent to visible light. This property is crucial for applications where light transmission is desired, such as in optical coatings or certain photovoltaic devices.

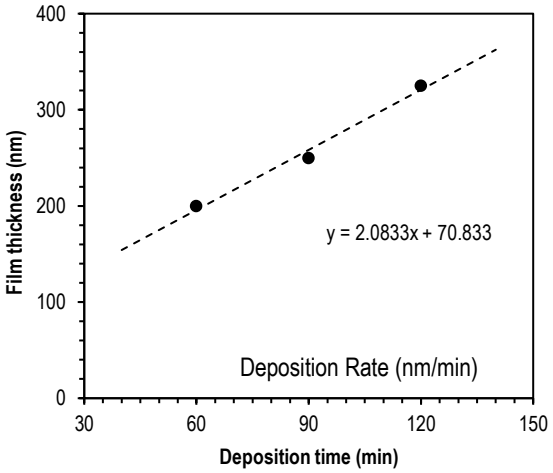

Fig. (1) Deposition rate of the DC reactive sputtering system used for the preparation of Al_2O_3 thin films

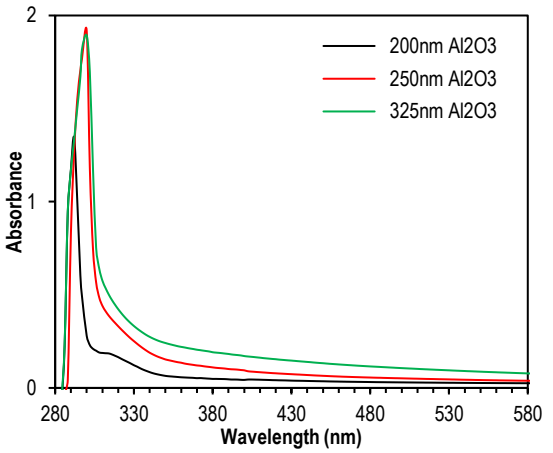

Fig. (2) Absorption spectra of the prepared samples in the UV and visible regions

Notably, the magnitude of the absorption peak and the overall absorbance throughout the observed wavelength range increase with increasing Al_2O_3 layer thickness. The 325 nm Al_2O_3 layer exhibits the highest absorbance, followed by the 250 nm layer, and then the 200 nm layer, which shows the lowest absorbance. This direct correlation between layer

thickness and absorbance is expected, as a thicker material provides more absorbing centers, leading to a higher probability of photon absorption. The gradual tailing off of the absorption curves into the longer wavelengths (visible region) might also indicate some degree of light scattering or defect-related absorption, which could be more pronounced in thicker films due to increased material volume and potential for structural imperfections. This detailed analysis of the absorption spectra provides valuable insights into the optical properties of these Al_2O_3/Si multilayer structures, highlighting their potential for applications requiring specific UV absorption and visible light transmission characteristics.

The photoluminescence (PL) spectra in Fig. (3) illustrate the emission characteristics of the prepared multilayer Al_2O_3/Si structures with varying Al_2O_3 layer thicknesses (200, 250, and 325 nm). A key feature across all spectra is the presence of multiple emission peaks, suggesting the involvement of several radiative recombination pathways within these structures. For the 200 nm Al_2O_3 sample (black curve), two distinct peaks are observed around 500 nm and 800 nm, indicating emission in both the green-yellow and near-infrared regions. The 250 nm Al_2O_3 sample (red curve) also exhibits two prominent peaks, but they are shifted to approximately 500 nm and 770 nm, with a significantly higher overall PL intensity compared to the 200 nm sample, particularly for the longer wavelength peak. This increase in intensity suggests that an optimal Al_2O_3 thickness around 250 nm might enhance radiative recombination processes. In contrast, the 325 nm Al_2O_3 sample (green curve) shows emission peaks around 550 nm and 830 nm. While the peak at 830 nm is quite strong, it is lower in intensity than the corresponding peak for the 250 nm sample, and the overall PL intensity is generally lower than that of the 250 nm sample across the spectrum.

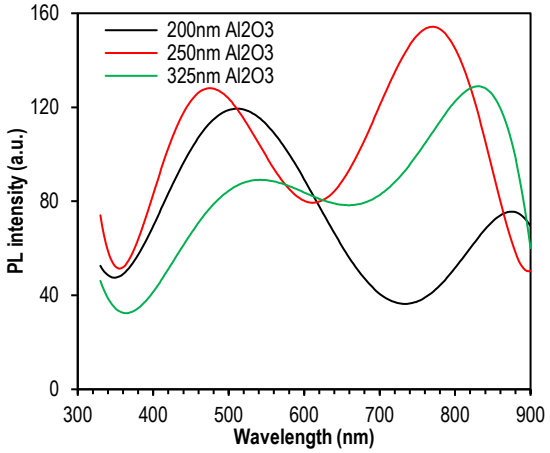

Fig. (3) Photoluminescence spectra of the prepared samples in the UV and visible regions

The shifts in peak positions and variations in intensity with Al_2O_3 thickness are indicative of quantum mechanical effects, such as quantum confinement, especially if silicon nanocrystals are formed within the Al_2O_3 matrix during fabrication. Interface quality between the Al_2O_3 and Si layers, as well as the presence of defects or oxygen vacancies within the Al_2O_3 film, can also significantly influence these PL characteristics. The observed oscillations in the spectra, particularly noticeable for the 250 nm and 325 nm samples, could also be attributed to interference effects within the multilayer structure, where emitted light undergoes constructive and destructive interference as it propagates through the different layers. These spectral variations provide crucial insights into the interplay between Al_2O_3 layer thickness, material defects, and optical properties in these multilayer structures.

4. Conclusions

In concluding remarks, the PL spectra indicate multiple emission peaks, suggesting various radiative recombination pathways. The 250 nm Al_2O_3 sample shows significantly higher PL intensity and distinct peak shifts compared to other thicknesses, implying an optimal thickness for enhancing radiative recombination. Shifts in peak positions and intensity variations with Al_2O_3 thickness are attributed to quantum mechanical effects, such as quantum confinement, and the influence of interface quality or defects. Oscillations in the PL spectra may also arise from interference effects within the multilayer structure. These findings underscore the critical interplay between Al_2O_3 layer thickness, material defects, and the resulting optical properties of these multilayer structures.

References

[1] P.M. Martin, **"Introduction to Surface Engineering and Functionally Engineered Materials"**, Ch. 6, John Wiley & Sons (NJ, 2011), p. 339.

[2] K. Seshan, **"Handbook of Thin Film Deposition: Techniques, Processes, and Technologies"**, 3rd ed., Ch. 4, William Andrew (Amsterdam, 2012).

[3] K.A. Al-Hamdani, "Current–voltage and capacitance-voltage characteristics of Se/Si heterojunction prepared by DC planar magnetron sputtering technique", *Iraqi J. Phys.*, 8(13) (2010) 97-100.

[4] M.K. Khalaf et al., "Operation Characteristics of a Closed-Field Unbalanced Dual-Magnetrons Plasma Sputtering System", *Bulg. J. Phys.*, 41(1) (2014) 24-33.

[5] K.A. Aadim, "Control the deposition uniformity using ring cathode by DC discharge technique", *Iraqi J. Phys.*, 15(32) (2017) 57-60.

[6] O.A. Hammadi, "Nanostructured CdSnSe Thin Films Prepared by DC Plasma Sputtering of Thermally Casted Targets", *Iraqi J. Appl. Phys.*, 14(4) (2018) 33-36.

[7] E.A. Al-Oubidy and F.J. Al-Maliki, "Effect of Gas Mixing Ratio on Energy Band Gap of Mixed-Phase Titanium Dioxide Nanostructures Prepared by Reactive Magnetron Sputtering Technique", *Iraqi J. Appl. Phys.*, 14(4) (2018) 19-23.

[8] M.A. Hameed and Z.M. Jabbar, "Optimization of Preparation Conditions to Control Structural Characteristics of Silicon Dioxide Nanostructures Prepared by Magnetron Plasma Sputtering", *Silicon*, 10(4) (2018) 1411-1418.

[9] M.S. Edan, "Copper Nitride Nanostructures Prepared by Reactive Plasma Sputtering Technique", *Iraqi J. Mater.*, 4(1) (2025) 31-36.

[10] R.A. Anaee et al., "Alumina Nanoparticle/Polypyrrole Coating for Carbon Steel Protection in Simulated Soil Solution", *Eng. Tech. J.*, 35(9A) (2017) 943-949.

[11] N. Zaim and O. Bayhatun, "A Study on the Gamma-Ray Attenuation Coefficients of Al_2O_3 and $Al_2O_3.TiO_2$ Compounds", Süleyman Demirel University Journal of Natural and Applied Sciences, 22 (2018) 312-318.

[12] M.K. Lambert et al., "Physical properties of γ–Al_2O_3 nanostructures prepared by high-temperature casting", *Mater. Eng. Technol.*, 25(1) (2020) 33-42.

[13] S.U. Ilyasa, R. Pendyalaa, and N. Marneni, "Stability and Agglomeration of Alumina Nanoparticles in Ethanol-Water Mixtures", *Procedia Eng.*, 148 (2016) 290-297.

[14] R. Darwesh et al., "Improved radiation shielding properties of epoxy resin composites using Sb_2O_3 and Al_2O_3 nanoparticles additives", *Annals Nucl. Ener.*, 200 (2024) 110385.

[15] F.J. Kadhim et al., "Fabrication of UV Photodetector from Nickel Oxide Nanoparticles Deposited on Silicon Substrate by Closed-Field Unbalanced Dual Magnetron Sputtering Techniques", *Opt. Quantum Electron.*, 47(12) (2015) 3805-3813.

[16] M.K. Khalaf et al., "Fabrication and Characterization of UV Photodetectors Based on Silicon Nitride Nanostructures Prepared by Magnetron Sputtering", *Proc. IMechE, Part N, J. Nanomater. Nanoeng. Nanosys.*, 230(1) (2016) 32-36.

[17] R.H. Turki and M.A. Hameed, "Spectral and Electrical Characteristics of Nanostructured NiO/TiO_2 Heterojunction Fabricated by DC Reactive Magnetron Sputtering", *Iraqi J. Appl. Phys.*, 16(3) (2020) 39-42.

[18] S.H. Faisal and M.A. Hameed, "Heterojunction Solar Cell Based on Highly-Pure Nanopowders Prepared by DC Reactive Magnetron Sputtering", *Iraqi J. Appl. Phys.*, 16(3) (2020) 27-32.

[19] A.Y. Bahlool, "Temperature-Dependent Optoelectronic Characteristics of p-SnO_2/n-Si Heterojunction Structures", *Iraqi J. Appl. Phys. Lett.*, 7(1) (2024) 23-26.

[20] D.A. Taher and M.A. Hameed, "Employment of Silicon Nitride Films Prepared by DC Reactive Sputtering Technique for Ion Release Applications", *Iraqi J. Phys.*, 21(3) (2023) 33-40.

[21] B.K. Nasser and M.A. Hameed, "Structural Characteristics of Silicon Nitride Nanostructures Synthesized by DC Reactive Magnetron Sputtering", *Iraqi J. Appl. Phys.*, 15(4) (2019) 33-36.

[22] A.N. Munif and F.J. Kadhim, "Structural Characteristics and Photocatalytic activity of TiO2/Si3N4 nanocomposite synthesized via plasma sputtering technique", *Iraqi J. Phys.*, 22(4) (2024) 99-106.

[23] N.A.H. Hashim and F.J. Kadhim, "Structural and Optical Characteristics of Co_3O_4 Nanostructures Prepared by DC Reactive Magnetron Sputtering", *Iraqi J. Appl. Phys.*, 18(4) (2022) 31-36.

[24] A.M. Hameed and M.A. Hameed, "Spectroscopic characteristics of highly pure metal oxide nanostructures prepared by DC reactive magnetron sputtering technique", *Emerg. Mater.*, 6 (2022) 627-633.

[25] D.A. Taher and M.A. Hameed, "Spectroscopic Characteristics of Silicon Nitride Thin Films Prepared by DC Reactive Sputtering Using Silicon targets with Different Types of Conductivity", *Iraqi J. Appl. Phys.*, 19(4A) (2023) 73-76.

[26] D.A. Taher and M.A. Hameed, "Structural and Hardness Characteristics of Silicon Nitride Thin Films Deposited on Metallic Substrates by DC Reactive Sputtering Technique", *Silicon*, 15 (2023) 7855-7864.

[27] M.A. Hameed et al., "Characterization of Multilayer Highly-Pure Metal Oxide Structures Prepared by DC Reactive Magnetron Sputtering", *Iraqi J. Mater.*, 3(4) (2024) 1-8.

[28] M.A. Hameed and Z.M. Jabbar, "Preparation and Characterization of Silicon Dioxide Nanostructures by DC Reactive Closed-Field Unbalanced Magnetron Sputtering", *Iraqi J. Appl. Phys.*, 12(4) (2016) 13-18.

[29] F.J. Al-Maliki et al., "Optimization of Rutile/Anatase Ratio in Titanium Dioxide Nanostructures prepared by DC Magnetron Sputtering Technique", *Iraqi J. Sci.*, 60(special issue) (2019) 91-98.

[30] F.J. Al-Maliki and E.A. Al-Oubidy, "Effect of gas mixing ratio on structural characteristics of titanium dioxide nanostructures synthesized by DC reactive magnetron sputtering", *Physica B: Cond. Matter*, 555 (2019) 18-20

[31] M.A. Hameed et al., "Characterization of Multilayer Highly-Pure Metal Oxide Structures Prepared by DC Reactive Magnetron Sputtering Technique", *Iraqi J. Appl. Phys.*, 16(4) (2020) 25-30

[32] A.M. Hameed and M.A. Hameed, "Highly-Pure Nanostructured Metal Oxide Multilayer Structure Prepared by DC Reactive Magnetron Sputtering Technique", *Iraqi J. Appl. Phys.*, 18(4) (2022) 9-14.

